



Use of Aloe vera shell ash supported $\text{Ni}_{0.5}\text{Zn}_{0.5}\text{Fe}_2\text{O}_4$ magnetic nanoparticles for removal of Pb (II) from aqueous solutions

Samira Namavari¹, Farid Moeinpour^{2*}

¹MSc in Water and Wastewater Engineering, Department Environmental Engineering, Faculty of Natural Resources, Islamic Azad University, Bandar Abbas Branch, Bandar Abbas, Iran

²Assistant Professor, Department of Chemistry, College of Science, Bandar Abbas Branch, Islamic Azad University, Bandar Abbas, Iran

Abstract

Background: Lead (Pb) is a heavy metal that is widely utilized in industries. It contaminates soil and groundwater. Its non-biodegradability, severe toxicity, carcinogenicity, ability to accumulate in nature and contaminate groundwater and surface water make this toxic heavy metal extremely dangerous to living beings and the environment. Therefore, technical and economic methods of removing Pb are of great importance. This study evaluated the efficiency of $\text{Ni}_{0.5}\text{Zn}_{0.5}\text{Fe}_2\text{O}_4$ magnetic nanoparticles supported by Aloe vera shell ash in removing Pb from aqueous environments.

Methods: The adsorbent was characterized by several methods, including x-ray diffraction (XRD), scanning electron microscopy (SEM), and Fourier transform infrared spectroscopy (FT-IR). Then, the potential of Aloe vera shell ash-supported $\text{Ni}_{0.5}\text{Zn}_{0.5}\text{Fe}_2\text{O}_4$ magnetic nanoparticles to adsorb Pb (II) was investigated. To determine the amount of lead absorbed by this adsorbent, different pHs (2, 4, 5, and 6), adsorbent doses (0.01–0.40 g), Pb concentrations (5, 10, 20, 30, 40, 50, 60, 80, 100, 200, 300, and 600 mg/L), and exposure times (0, 5, 10, 15, 20, 30, 40, 50, and 60 minutes until reaching equilibrium) were tested using an atomic absorption spectrometer (Varian-AA240FS). Residual concentrations of Pb were read.

Results: The results show that a time of 15 minutes, pH value of 9, and adsorbent dose of 0.2 g are the optimum conditions for Pb (II) removal by this adsorption process. Increasing the initial concentration of Pb (II) from 5 to 600 mg/L decreased removal efficiency from 98.8% to 73%. The experimental data fit well into the Freundlich isotherm model ($R^2 = 0.989$).

Conclusion: $\text{Ni}_{0.5}\text{Zn}_{0.5}\text{Fe}_2\text{O}_4$ magnetic nanoparticles supported by Aloe vera shell ash comprise a low-cost, simple, and environmentally benign procedure. The maximum monolayer adsorption capacity based on the Langmuir isotherm ($R^2 = 0.884$) is 47.2 mg g^{-1} . The prepared magnetic adsorbent can be well dispersed in aqueous solutions and easily separated from them with the aid of an external magnet after adsorption. The process for purifying water presented here is clean and safe. Therefore, this adsorbent is applicable to managing water pollution caused by Pb (II) ions.

Keywords: Adsorption, Pb (II) ions, $\text{Ni}_{0.5}\text{Zn}_{0.5}\text{Fe}_2\text{O}_4$, Aloe vera, Aqueous solutions

Citation: Namavari S, Moeinpour F. Use of Aloe vera shell ash supported $\text{Ni}_{0.5}\text{Zn}_{0.5}\text{Fe}_2\text{O}_4$ magnetic nanoparticles for removal of Pb (II) from aqueous solutions. Environmental Health Engineering and Management Journal 2016; 3(1): 15–21.

Article History:

Received: 10 January 2016

Accepted: 31 January 2016

ePublished: 12 February 2016

*Correspondence to:

Farid Moeinpour

Email: f.moeinpour@gmail.com

Introduction

Adsorption has been established as an important and economically practical treatment technology for removing Pb (II) ions from water and wastewater. Activated carbon is the adsorbent most commonly used for removing Pb (II) ions from aqueous solution. Despite the abundance of applications for activated carbon, its uses are sometimes limited by its high cost and loss during re-formation (1). Therefore, researchers are seeking new low-cost substitute adsorbents for water pollution control, especially where cost plays an important role. Many efforts have been made toward the development of other adsorbents that are effective and inexpensive. They can be produced from a wide variety of raw materials which are abundant

and have high carbon and low inorganic content. Owing to the low cost and high accessibility of these materials, it is not essential to have complex regeneration processes. Such inexpensive adsorption methods have attracted the attention of many researchers. Often, the adsorption capabilities of such adsorbents are not great; therefore, studies of more and more new adsorbents are still being developed. Some inexpensive adsorbents for the removal of Pb (II) ions that have been studied are modified agricultural waste (2), hazelnut husks (3), *Moringa oleifera* seed powder (1), olive waste (3), waste coconut buttons (4), magnetically modified tea (5), activated carbon prepared from saffron leaves (6), bael leaves (7), pomegranate peel (1), multi-walled carbon nanotube magnetic composites (8),



marine green algae (9), tourmaline (1), amino-functionalized Fe_3O_4 magnetic nanoparticles (10), $\text{Fe}_3\text{O}_4@\text{SiO}_2\text{-NH}_2$ (11), waste maize bran (12), coir (13), *Caulerpa lentillifera* (14), Fraxinus tree leaves (15), lignin (16), rice husk ash (17), corn cobs (18), *Moringa oleifera* bark (19), and others. In recent years, economic problems have encouraged the creation of inexpensive, efficient alternative methods of wastewater treatment. One of the most efficient, technical, and economic methods is the use of magnetic adsorbents. These adsorbents have magnetic properties and, by using an external magnetic field, can be easily separated from solutions. In magnetic separation, the usual high costs of separation, e.g., centrifugation and filtration, are not incurred (20). Extensive research has been done in the field of magnetization of materials such as chitosan (21), silica (22), polymer (23), and activated carbon (24) for water contaminants removal. The use of this property in nanoparticles, due to their high specific surface area and adsorption capacities, is very good (25-27). Nickel-zinc ferrites have drawn noticeable consideration from researchers because of their remarkable magnetic properties, large permeability, and very high electrical resistivity (28). They have an extensive list of potential applications in such areas as high-density information storage devices, microwave devices, transformer cores, magnetic fluids, etc. (29). There are many applications for activated carbon in removing chlorine, separating gases, air pollution treatment, and recycling heavy metals from aqueous solutions. However, because of the high cost, alternative options have been suggested. Ash, due to its low cost of production, is a good alternative to activated carbon (30-34). Ash can be produced from a wide range of carbon materials, including wood, coal, shell, walnut shell, fruit stones, agricultural waste, etc (35).

This study investigated the capability of $\text{Ni}_{0.5}\text{Zn}_{0.5}\text{Fe}_2\text{O}_4$ magnetic nanoparticles that were surface-modified with ash prepared from Aloe vera shell ($\text{Ni}_{0.5}\text{Zn}_{0.5}\text{Fe}_2\text{O}_4/\text{ASA}$) as a low-cost adsorbent for the removal of Pb (II) ions from aqueous solutions and studied the adsorption mechanism of Pb (II) ions onto this adsorbent.

Methods

Analytical-grade salt $\text{Pb}(\text{NO}_3)_2$ was obtained from Merck. A 1000 mg/L stock solution of the salt was prepared in deionized water. All working solutions were made by consecutive diluting with deionized water. Deionized water was prepared using a Millipore Milli-Q (Bedford, MA) water purification system. All reagents ($\text{Fe}(\text{NO}_3)_3 \cdot 9\text{H}_2\text{O}$, $\text{Zn}(\text{NO}_3)_2 \cdot 6\text{H}_2\text{O}$ and $\text{Ni}(\text{NO}_3)_2 \cdot 6\text{H}_2\text{O}$, NaOH and HNO_3) used in the study were of analytical grade and purchased from Aldrich. X-ray diffraction (XRD) analysis was carried out using a PAN analytical X'Pert Pro x-ray diffractometer. Surface morphology and particle size were investigated with a Hitachi S-4800 scanning electron microscopy (SEM) instrument. FT-IR spectra were determined as KBr pellets on a Bruker model 470 spectrophotometer. All the metal ion concentrations were measured with a Varian AA240FS atomic absorption spectrophotometer.

Aloe vera is grown in southern Iran. Aloe vera shell was collected from Qeshm Island, Hormozgan, Iran, and was applied as a raw material for the preparation of surface-modified adsorbent. The collected Aloe vera shells were washed and dried in an air oven at 80°C for 24 hours and then ground and sieved to the desired particle size (2-3 mm). The resultant sieved powder was carbonized in a furnace at 700°C , at a heating rate of $10^\circ\text{C}/\text{min}$ for 2 hours. The method used to produce carbon materials was similar to that used in other studies (36).

Synthesis of $\text{Ni}_{0.5}\text{Zn}_{0.5}\text{Fe}_2\text{O}_4/\text{ASA}$

Ni-Zn ferrite was prepared using stoichiometric ratios of metal nitrates and freshly extracted egg white (37). The metal nitrates ($\text{Fe}(\text{NO}_3)_3 \cdot 9\text{H}_2\text{O}$, $\text{Zn}(\text{NO}_3)_2 \cdot 6\text{H}_2\text{O}$ and $\text{Ni}(\text{NO}_3)_2 \cdot 6\text{H}_2\text{O}$) and 2 g ASA were dissolved together in a minimum amount of double-distilled water to get a clear solution. Sixty milliliters of extracted egg white dissolved in 40 mL of double-distilled water while being vigorously stirred was added to the nitrate mixture at the ambient temperature. After constant stirring for 30 minutes, the resultant sol-gel was evaporated at 80°C until the dry precursor was obtained. The dried precursors were ground and calcined in a muffle furnace at 550°C for 2 hours.

Adsorption experiments

Batch adsorption of lead ions onto the adsorbent ($\text{Ni}_{0.5}\text{Zn}_{0.5}\text{Fe}_2\text{O}_4/\text{ASA}$) was investigated in aqueous solutions under various operating conditions viz. pH 2–6, at a temperature of 298 K, for an initial Pb (II) ion concentration of 50 mg/L. About 0.20 g adsorbent was added to 50 mL of lead nitrate solution (50 mg/L). Then the mixture was agitated on a shaker at 250 rpm. The initial pH values of the lead solutions were adjusted from 2 to 6 with 0.1 mol/L HNO_3 or 0.1 mol/L NaOH solutions using a pH meter. After equilibrium was reached, the samples were centrifuged and the adsorbent ($\text{Ni}_{0.5}\text{Zn}_{0.5}\text{Fe}_2\text{O}_4/\text{ASA}$) was magnetically removed from the solution. The concentration of Pb (II) in the supernatant was measured by flame atomic absorption spectrometry. The effects of several parameters, such as contact time, initial concentration, pH, and adsorbent dose, on the extent of Pb (II) adsorption were investigated.

The Pb (II) removal percentage was calculated using Eq. (1):

$$\text{Removal \%} = \frac{C_0 - C_t}{C_0} \times 100 \quad (1)$$

where C_0 and C_t (mg/L) are the Pb (II) concentrations in the solution at initial and equilibrium time, respectively. The amount of Pb (II) adsorbed (Q_e) was calculated using Eq. (2):

$$Q_e = \frac{(C_0 - C_e)V}{m} \quad (2)$$

where C_0 and C_e are, respectively, the initial and equilibrium concentrations of Pb (II) (mg/L), m is the mass of adsorbent (g), and V is the volume of solution (L).

Adsorption isotherms

Adsorption isotherms were obtained using 0.20 g of adsorbent and 50 mL of Pb (II) solution with different concentrations (50-600 mg/L) at 298 K. These solutions were buffered at an optimum pH (pH = 5) for adsorption and agitated on a shaker at 250 rpm until they reached adsorption equilibrium (15 minutes). The quantity of Pb (II) adsorbed was derived from the change in concentration.

Results

In this section, the results of this study are presented in the form of diagrams and tables. Ni_{0.5}Zn_{0.5}Fe₂O₄/ASA nanocrystallites were characterized by FT-IR (Figure 1), XRD (Figure 2), and SEM (Figure 3).

Figure 4 shows the different sampling times, the concentration of Pb remaining, and the adsorption balance time. As shown in Figure 4, removal efficiency increased in the time range of 0 to 15 minutes and became fixed and partly decreased at 15 to 60 minutes. Thus, the adsorption balance time was determined to be 15 minutes in this test.

The effect of solution pH on Pb (II) adsorption was studied at pH 2–6 at 298 K. As shown in Figure 5, the adsorption rate of Pb (II) was enhanced by increasing pH values from 2 to 6. Figure 5 shows the removal efficiency of lead at the balance time and at 4 different pHs (2, 4, 5, and 6), equaling, respectively, 99.2%, 99.4%, 99.8%, and 99.2%. Maximum adsorption occurred at around pH 5.0, and this value was therefore selected for all adsorption experiments in this study.

The effect of change in the adsorbent amount on the process of Pb (II) adsorption was investigated with different

adsorbent doses in the range of 0.01-0.40 g. The results are shown in Figure 6. The best removal of Pb (II) is at about 99.8%, using an adsorbent dosage of 0.20 g in 50 mL of 50 mg/L Pb (II) solution.

Batch adsorption experiments were performed at different initial Pb (II) concentrations (5, 10, 20, 30, 40, 50, 60, 80, 100, 200, 300, and 600 mg/L), while other experimental parameters were kept constant. Figure 7 shows that the adsorption capacity of Pb (II) increased, but the removal percent (%R) of Pb (II) decreased when initial concentra-

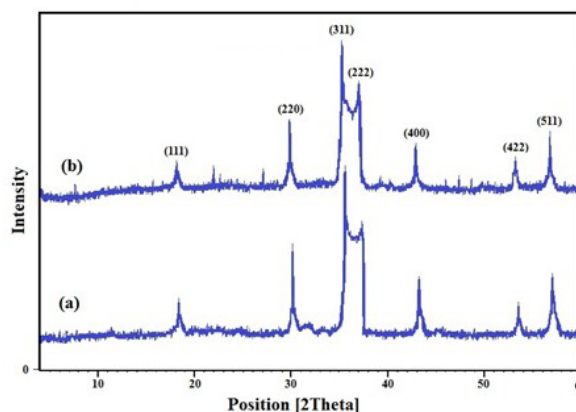


Figure 2. XRD patterns of Ni_{0.5}Zn_{0.5}Fe₂O₄. (a) Synthesized Ni_{0.5}Zn_{0.5}Fe₂O₄; (b) Standard Ni_{0.5}Zn_{0.5}Fe₂O₄ (JCPDS 08-0234).

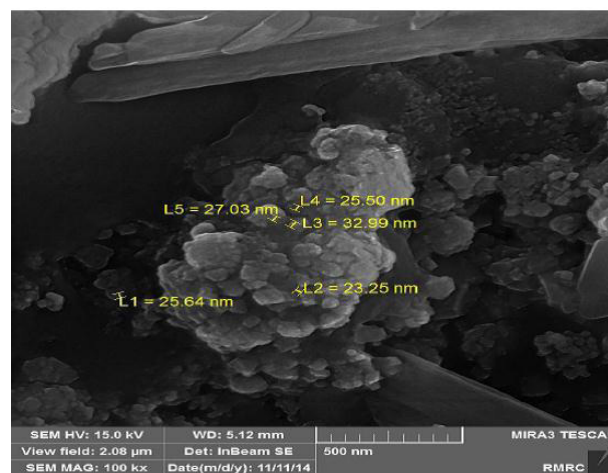


Figure 3. SEM image of Ni_{0.5}Zn_{0.5}Fe₂O₄/ASA nanocomposite.

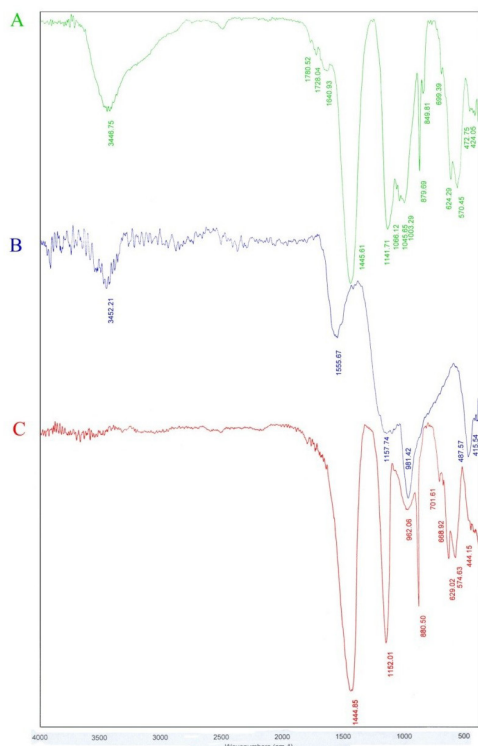


Figure 1. The FTIR spectra of: (A) Ni_{0.5}Zn_{0.5}Fe₂O₄/ASA; (B) ASA; (C) Ni_{0.5}Zn_{0.5}Fe₂O₄

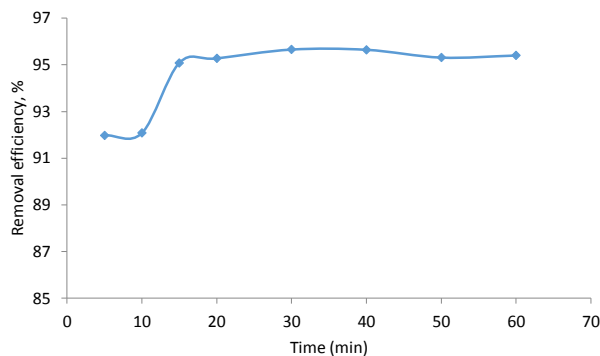


Figure 4. Effect of contact time

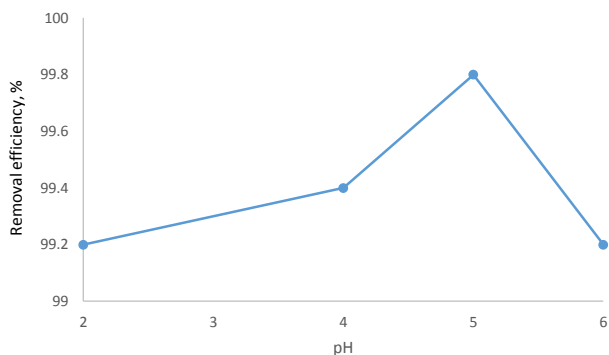


Figure 5. Effect of pH on Pb (II).

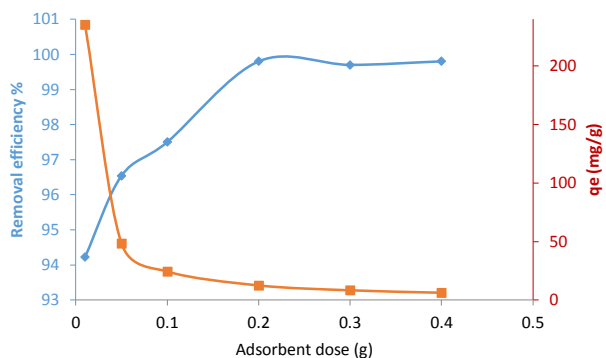


Figure 6. The effect of adsorbent dosage.

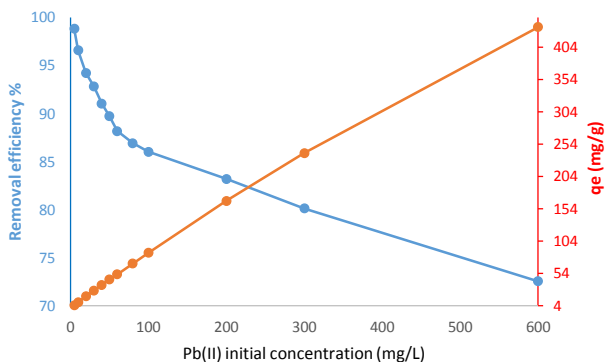


Figure 7. Effect of initial Pb (II) concentration

tion was increased, indicating that the adsorption of Pb (II) on to Ni_{0.5}Zn_{0.5}Fe₂O₄/ASA is highly related to initial Pb (II) concentration.

The adsorption isotherms of Pb (II) by the adsorbent are shown in Table 1. In Table 1, R² = 0.884 in the Langmuir model, R² = 0.989 in the Freundlich model, and R² = 0.650

in the Dubinin–Radushkevich model.

Discussion

Ni_{0.5}Zn_{0.5}Fe₂O₄ nanocrystallites were prepared according to the procedure reported by Gabal et al (39). Ni_{0.5}Zn_{0.5}Fe₂O₄/ASA nano-crystallites were characterized by FT-IR (Figure 1), XRD (Figure 2), and SEM (Figure 3). In the FT-IR spectrum of Ni_{0.5}Zn_{0.5}Fe₂O₄/ASA (Figure 1A), many of the bands of Ni_{0.5}Zn_{0.5}Fe₂O₄ (Figure 1C) and ASA (Figure 1B), with a slight shift for some of them, are distinct, which shows that ASA has been well supported on the Ni_{0.5}Zn_{0.5}Fe₂O₄. The bands in the low-frequency region (1000-500 cm⁻¹) were caused by the iron oxide framework, which is in accordance with the magnetite spectrum. The peak at 1440.85 cm⁻¹ is related to the Fe–O bond (33). In Figure 1A, the presence of the –OH stretching mode is evidenced by the peak close to 3446 cm⁻¹. To verify the formation of Ni-Zn ferrite in the prepared magnetic nanoparticles, the XRD pattern of the sample was investigated. The XRD patterns (Figure 2) show that Ni_{0.5}Zn_{0.5}Fe₂O₄ nanoparticles have a spinal framework with all the main peaks compatible the Ni_{0.5}Zn_{0.5}Fe₂O₄ standard pattern (JCPDS 08-0234). The adsorbent particle size was investigated using SEM. The SEM photograph of the sample (Figure 3) shows that the average size of Ni_{0.5}Zn_{0.5}Fe₂O₄/ASA is slightly less than 100 nm.

The effect of contact time on the amount of Pb (II) adsorbed was studied at 50 mg/L initial concentration of lead. It can be observed from Figure 4 that the percentage of adsorptions increased with increases in contact time. Minimum adsorption was 92.0% for the time of 5 minutes, and maximum adsorption was 95.1% for the time of 15 minutes. The adsorption characteristic indicated a rapid uptake of the lead. The adsorption rate, however, diminished to a constant value as contact time was increased, because all available sites were covered and no active site was present for adsorbing.

The acidity of the aqueous solution applies a considerable effect on the adsorption process, because it can alter the solution chemistry of contaminants and the state of functional groups on the surface of adsorbents (39, 40). However, at low pH values, hydrogen ions (H⁺) were likely to compete with Pb (II) and thus lower the amount of Pb (II) removed. Therefore, the great Pb (II) adsorption occurring at higher pHs could be ascribed to a decrease in competition between H⁺ and Pb (II) at the same adsorption site of the adsorbent beads. At a pH value of 5.9, the

Table 1. Langmuir, Freundlich, D–R isotherm constants for the adsorption of Pb (II) ions onto Ni_{0.5}Zn_{0.5}Fe₂O₄/ASA

Langmuir			
q _m (mg g ⁻¹)	K _L	R _L	R ²
47.2	1.91	8.72 × 10 ⁻⁴	0.884
Freundlich			
1/n	K _F		R ²
0.50	1.93		0.989
Dubinin–Radushkevich (D–R)			
q _m (mg g ⁻¹)	β (mol ² kJ ⁻²)	R ²	E (kJ mol ⁻¹)
6.7	7 × 10 ⁻⁸	0.650	2.673

Pb (II) ions begin to hydrolyze and then form a small number of Pb(OH)₂ or Pb(OH)₃ varieties (41). Compared with Pb (II) ions, these species are unfavorable for adsorption, which accounts for the little reduction in adsorption capacity. Therefore, maximum adsorption occurred at around pH 5.0, and this value was therefore selected for all adsorption experiments in this study. The results are in line with the findings of Zhang et al (14) on the removal of Pb (II) by Fe₃O₄@SiO₂-NH₂ core-shell nanomaterials. From Figure 6, it can be seen that as the adsorbent dose is increased, the percentage of removal also increased until it approached a saturation point, where increases in adsorbent dose did not alter the percentage of removal. An increase in adsorption rate with adsorbent quantity can be ascribed to increased surface area and the availability of more adsorption sites.

Batch adsorption experiments were performed at different initial Pb (II) concentrations. As shown in Figure 7, these observations can be explained by considering the fact that increasing the initial Pb²⁺ concentration made more Pb²⁺ ions available, while the amount of active sites on the adsorbent remained constant which led to a lower %R.

Isotherm studies can explain how an adsorbate interacts with an adsorbent. The experimental data corresponded with the Langmuir, Freundlich and Dubinin-Radushkevich models as shown in Table 1.

The Langmuir isotherm model, which defines a monolayer adsorption, is given in Eq. (3):

$$\frac{1}{q_e} = \frac{1}{K_L q_m} \frac{1}{C_e} + \frac{1}{q_m} \quad (3)$$

where q_e = the amount of Pb (II) adsorbed per unit mass at equilibrium (mg/g);

q_m = the maximum amount of adsorbent that can be adsorbed per unit mass adsorbent (mg/g);

C_e = concentration of adsorbent (in the solution at equilibrium) (mg/L);

K_L = adsorption equilibrium constant.

A plot of 1/q_e versus 1/C_e gives a straight line with a slope of 1/K_Lq_m and intercept 1/q_m.

The main characteristics of the Langmuir isotherm can be expressed in terms of a dimensionless constant separation factor R_L that is given by Eq. (4) (42):

$$R_L = \frac{1}{1 + K_L C_0} \quad (4)$$

Where C₀ is the highest initial concentration of adsorbate (mgL⁻¹), and K_L (Lmg⁻¹) is the Langmuir constant. The value of R_L shows the shape of the isotherm to be either unfavorable (R_L > 1), linear (R_L = 1), favorable (0 < R_L < 1), or irreversible (R_L = 0). The R_L values between 0 and 1 indicate favorable adsorption. In this study, the value of R_L is 0.116, which shows the favorable adsorption of Pb (II) by Ni_{0.5}Zn_{0.5}Fe₂O₄/ASA.

The Freundlich isotherm is expressed by Eq. (5). This isotherm model defines a heterogeneous adsorption with different surface energy sites and supposes the change of uptake with exponential distribution of adsorption sites

and energies (43-45).

$$\log q_e = \log K_F + \frac{1}{n} \log C_e \quad (5)$$

where C_e (mg/L) and q_e (mg/g) are the equilibrium concentration of adsorbent in the solution and the amount of adsorbent adsorbed at equilibrium, respectively; K_F (mg^{1-(1/n)} L^{1/n} g⁻¹) and n are the Freundlich constant which indicates the adsorption capacity for the adsorbent and adsorption intensity, respectively.

A graph of log q_e versus log C_e provides a straight line with slope 1/n and intercept log K_F. The value of 1/n identifies the adsorption intensity and type of isotherm as favorable (0.1 < 1/n < 0.5) or unfavorable (1/n > 2). The Freundlich parameter 1/n is related to the adsorption intensity of the adsorbent. When 0.1 < 1/n ≤ 0.5, the adsorption of the adsorbate is easy; when 0.5 < 1/n ≤ 1, the adsorption process is difficult; when 1/n > 1, adsorption takes place with much difficulty (46, 47). In the current study, the value of 1/n (0.43) shows the favorable adsorption of Pb (II) onto Ni_{0.5}Zn_{0.5}Fe₂O₄/ASA.

In order to discern between physical and chemical adsorption, the sorption data was analyzed using the Dubinin-Radushkevich (D-R) equation, which is given in Eq. (6):

$$\ln q_e = \ln q_m - \beta \varepsilon^2 \quad (6)$$

where β is a constant related to the mean energy of adsorption (mol² kJ⁻²), q_m is the maximum adsorption capacity of metal ions (mg g⁻¹), and ε is the Polanyi potential given by Eq. (7):

$$\varepsilon = RT \ln \left(1 + \frac{1}{C_e} \right) \quad (7)$$

where R is the gas constant (8.314 J mol⁻¹ K⁻¹) and T is the temperature (K). By plotting lnq_e versus ε² with experimental data, a straight line is obtained. From the intercept and slope, the values of q_m and β are determined. With the value of β, the mean energy E, which is the free energy transfer of one mole of solute from infinity to the surface of adsorbent, can be obtained using Eq. (8):

$$E = \frac{1}{\sqrt{2\beta}} \quad (8)$$

For E < 8 kJ mol⁻¹, the adsorption process might be performed physically, while chemical adsorption occurs when E > 8 kJ mol⁻¹(45).

All parameters are listed in Table 1. Looking at Table 1, in which the Langmuir, Freundlich, and D-R isotherm constants for the adsorption of Pb (II) are summarized, it can be derived from R² that the Freundlich model matched the experimental data better than either the Langmuir or D-R model. The research conducted by Senthil Kumar et al (3) on the removal of Pb (II) from aqueous solutions using chemically modified agricultural waste showed that the Freundlich model is a better fit in comparison with Langmuir. Moreover, it is clear that the adsorption of Pb (II) by Ni_{0.5}Zn_{0.5}Fe₂O₄/ASA may be explained as a physical

Table 2. Maximum adsorption capacity of different adsorbents for Pb (II) removal

Adsorbents	q_m (mg/g)	References
Modified agricultural waste	166.67	(46)
Hazelnut husk	109.90	(47)
Olive waste	6.57	(13)
Magnetically modified tea	44.50	(3)
Bael leaves	104.00	(4)
Marine green algae	15.62	(6)
Tourmaline	108	(48)
Amino-functionalized Fe_3O_4 magnetic nano-particles	40.10	(9)
$Fe_3O_4@SiO_2-NH_2$	243.90	(11)
Waste maize bran	142.86	(12)
Coir	48.83	(13)
Rice husk ash	91.74	(14)
Corncoobs	43.40	(15)
$Ni_{0.5}Zn_{0.5}Fe_2O_4/ASA$	47.20	This study

adsorption process, for the value of E is 2.673 kJ.

Adsorption capacity is a significant parameter which determines the performance of an adsorbent. Table 2 compares the maximum adsorption capacity of $Ni_{0.5}Zn_{0.5}Fe_2O_4/ASA$ for Pb (II) adsorption with that of other adsorbents in the literature.

Conclusion

$Ni_{0.5}Zn_{0.5}Fe_2O_4/ASA$ magnetic nanoparticles were used in the adsorption of Pb (II) ions from aqueous solutions. Maximum Pb (II) adsorption was achieved at pH 5 with a maximum adsorption capacity of 47.20 mgg^{-1} at 298 K. The adsorption isotherm fit the Freundlich model well. The prepared magnetic adsorbent can be well dispersed in the aqueous solution and easily separated from it with the aid of an external magnet after adsorption. The water treatment described here is clean and safe using magnetic nanoparticles. Thus, this adsorbent was found to be useful and valuable for controlling water pollution due to Pb (II) ions.

Acknowledgments

The authors acknowledge the Islamic Azad University-Bandar Abbas Branch for its financial support of this study.

Ethical issues

The authors hereby certify that all data collected during the study are as stated in this manuscript, and no data from the study has been or will be published elsewhere separately.

Competing interests

The authors declare that they have no competing interests.

Authors' contributions

All authors contributed equally and were involved in designing the study, data collection, and article approval.

References

1. El-Ashtoukhy ES, Amin N, Abdelwahab O. Removal of lead (II) and copper (II) from aqueous solution using pomegranate peel as a new adsorbent. *Desalination* 2008; 223(1-3): 162-73.
2. Baysal Z, Cinar E, Bulut Y, Alkan H, Dogru M. Equilibrium and thermodynamic studies on biosorption of Pb (II) onto *Candida albicans* biomass. *J Hazard Mater* 2009; 161(1): 62-7.
3. Senthil Kumar P, Senthamarai C, Sai Deepthi A, Bharani R. Adsorption isotherms, kinetics and mechanism of Pb (II) ions removal from aqueous solution using chemically modified agricultural waste. *Can J Chem Eng* 2013; 91(12): 1950-6.
4. Imamoglu M, Şahin H, Aydın Ş, Tosunoğlu F, Yılmaz H, Yıldız SZ. Investigation of Pb (II) adsorption on a novel activated carbon prepared from hazelnut husk by K_2CO_3 activation. *Desalination and Water Treatment* 2016; 57(10): 4587-96.
5. Prasad M, Freitas H. Removal of toxic metals from solution by leaf, stem and root phytomass of *Quercus ilex* L. (holly oak). *Environ Pollut* 2000; 110(2): 277-83.
6. Blázquez G, Calero M, Hernáinz F, Tenorio G, Martín-Lara M. Equilibrium biosorption of lead (II) from aqueous solutions by solid waste from olive-oil production. *Chem Eng J* 2010; 160(2): 615-22.
7. Anirudhan T, Sreekumari S. Adsorptive removal of heavy metal ions from industrial effluents using activated carbon derived from waste coconut buttons. *J Environ Sci* 2011; 23(12): 1989-98.
8. Akar T, Tunali S, Kiran I. *Botrytis cinerea* as a new fungal biosorbent for removal of Pb (II) from aqueous solutions. *Biochem Eng J* 2005; 25(3): 227-35.
9. Chakravarty S, Mohanty A, Sudha TN, Upadhyay A, Konar J, Sircar J, et al. Removal of Pb (II) ions from aqueous solution by adsorption using bael leaves (*Aegle marmelos*). *J Hazard Mater* 2010; 173(1-3): 502-9.
10. Shao D, Chen C, Wang X. Application of polyaniline and multiwalled carbon nanotube magnetic composites for removal of Pb (II). *Chem Eng J* 2012; 185-186: 144-50.
11. Jeyakumar RS, Chandrasekaran V. Adsorption of lead (II) ions by activated carbons prepared from marine green algae: equilibrium and kinetics studies. *International Journal of Industrial Chemistry* 2014; 5(1): 1-9.
12. Wang C, Wu J, Sun H, Wang T, Liu H, Chang Y. Adsorption of Pb (II) ion from aqueous solutions by tourmaline as a novel adsorbent. *Ind Eng Chem Res* 2011; 50(14): 8515-23.
13. Tan Y, Chen M, Hao Y. High efficient removal of Pb (II) by amino-functionalized Fe_3O_4 magnetic nano-particles. *Chem Eng J* 2012; 191: 104-11.
14. Zhang J, Zhai S, Li S, Xiao Z, Song Y, An Q, et al. Pb (II) removal of $Fe_3O_4@SiO_2-NH_2$ core-shell nanomaterials prepared via a controllable sol-gel process. *Chem Eng J* 2013; 215-216: 461-71.
15. Singh K, Talat M, Hasan S. Removal of lead from aqueous solutions by agricultural waste maize bran. *Bioresour Technol* 2006; 97(16): 2124-30.
16. Conrad K, Hansen HC. Sorption of zinc and lead on coir. *Bioresour Technol* 2007; 98(1): 89-97.
17. Apiratikul R, Pavasant P. Batch and column studies of biosorption of heavy metals by *Caulerpa lentillifera*. *Bioresour Technol* 2008; 99(8): 2766-77.
18. Sangi MR, Shahmoradi A, Zolgharnein J, Azimi GH,

- Ghorbandoost M. Removal and recovery of heavy metals from aqueous solution using *Ulmus carpinifolia* and *Fraxinus excelsior* tree leaves. *J Hazard Mater* 2008; 155(3): 513-22.
19. Guo X, Zhang S, Shan XQ. Adsorption of metal ions on lignin. *J Hazard Mater* 2008; 151(1): 134-42.
 20. Naiya TK, Bhattacharya AK, Mandal S, Das SK. The sorption of lead (II) ions on rice husk ash. *J Hazard Mater* 2009; 163(2-3): 1254-64.
 21. Tan G, Yuan H, Liu Y, Xiao D. Removal of lead from aqueous solution with native and chemically modified corncobs. *J Hazard Mater* 2010; 174(1-3): 740-5.
 22. Reddy DHK, Seshaiiah K, Reddy A, Rao MM, Wang M. Biosorption of Pb^{2+} from aqueous solutions by *Moringa oleifera* bark: equilibrium and kinetic studies. *J Hazard Mater* 2010; 174(1-3): 831-8.
 23. Shen Y, Tang J, Nie Z, Wang Y, Ren Y, Zuo L. Preparation and application of magnetic Fe_3O_4 nanoparticles for wastewater purification. *Sep Purif Technol* 2009; 68(3): 312-9.
 24. Cho DW, Jeon BH, Chon CM, Kim Y, Schwartz FW, Lee ES, et al. A novel chitosan/clay/magnetite composite for adsorption of Cu (II) and As (V). *Chem Eng J* 2012; 200-202: 654-62.
 25. Shi G, Sun B, Jin Z, Liu J, Li M. Synthesis of SiO_2/Fe_3O_4 nanomaterial and its application as cataluminescence gas sensor material for ether. *Sensors and Actuators B: Chemical* 2012; 171-172: 699-704.
 26. Dallas P, Georgakilas V, Niarchos D, Komninou P, Kehagias T, Petridis D. Synthesis, characterization and thermal properties of polymer/magnetite nanocomposites. *Nanotechnology* 2006; 17(8): 2046-53.
 27. Mohan D, Sarswat A, Singh VK, Alexandre-Franco M, Pittman CU Jr. Development of magnetic activated carbon from almond shells for trinitrophenol removal from water. *Chem Eng J* 2011; 172(2-3): 1111-25.
 28. Mak SY, Chen DH. Binding and sulfonation of poly (acrylic acid) on Iron oxide nanoparticles: a novel, magnetic, strong acid cation nano-adsorbent. *Macromol Rapid Commun* 2005; 26(19): 1567-71.
 29. Nitayaphat W, Jintakosol T. Removal of silver (I) from aqueous solutions by chitosan/carbon nanotube nanocomposite beads. *Advanced Materials Research* 2014; 893: 166-9.
 30. Nitayaphat W, Jintakosol T. Removal of silver (I) from aqueous solutions by chitosan/bamboo charcoal composite beads. *Journal of Cleaner Production* 2015; 87: 850-5.
 31. Sharma S, Verma K, Chaubey U, Singh V, Mehta B. Influence of Zn substitution on structural, microstructural and dielectric properties of nanocrystalline nickel ferrites. *Materials Science and Engineering: B* 2010; 167(3): 187-92.
 32. Virden A, O'Grady K. Structure and magnetic properties of Ni-Zn ferrite nanoparticles. *J Magn Magn Mater* 2005; 290: 868-70.
 33. Mane S, Vanjara A, Sawant M. Removal of phenol from wastewater using date seed carbon. *Journal of the Chinese Chemical Society* 2005; 52(6): 1117-22.
 34. Panday K, Prasad G, Singh V. Copper (II) removal from aqueous solutions by fly ash. *Water Res* 1985; 19(7): 869-73.
 35. Vázquez-Rivera NI, Soto-Pérez L, St John JN, Molina-Bas OI, Hwang SS. Optimization of pervious concrete containing fly ash and iron oxide nanoparticles and its application for phosphorus removal. *Constr Build Mater* 2015; 93: 22-8.
 36. Al. Haddabi M, Ahmed M, Al. Jebri Z, Vuthaluru H, Znad H, Al. Kindi M. Boron removal from seawater using date palm (*Phoenix dactylifera*) seed ash. *Desalination and Water Treatment* 2016; 57(11): 5130-7.
 37. Agrafioti E, Kalderis D, Diamadopoulos E. Arsenic and chromium removal from water using biochars derived from rice husk, organic solid wastes and sewage sludge. *J Environ Manage* 2014; 133: 309-14.
 38. Banat F, Al-Asheh S, Al-Makhadmeh L. Evaluation of the use of raw and activated date pits as potential adsorbents for dye containing waters. *Process Biochem* 2003; 39(2): 193-202.
 39. Gabal M, El-Shishtawy RM, Al Angari Y. Structural and magnetic properties of nano-crystalline Ni-Zn ferrites synthesized using egg-white precursor. *J Magn Magn Mater* 2012; 324(14): 2258-64.
 40. Pol VG, Daemen LL, Vogel S, Chertkov G. Solvent-free fabrication of ferromagnetic Fe_3O_4 octahedra. *Ind Eng Chem Res* 2009; 49(2): 920-4.
 41. Huang M-R, Li S, Li X-G. Longan shell as novel biomacromolecular sorbent for highly selective removal of lead and mercury ions. *J Phys Chem B* 2010; 114(10) 3534-42.
 42. Hall KR, Eagleton LC, Acrivos A, Vermeulen T. Pore-and solid-diffusion kinetics in fixed-bed adsorption under constant-pattern conditions. *Industrial & Engineering Chemistry Fundamentals* 1966; 5(2): 212-23.
 43. Chen H, Zhao J, Wu J, Dai G. Isotherm, thermodynamic, kinetics and adsorption mechanism studies of methyl orange by surfactant modified silkworm exuviae. *J Hazard Mater* 2011; 192(1): 246-54.
 44. Hou MF, Ma CX, Zhang WD, Tang XY, Fan YN, Wan HF. Removal of rhodamine B using iron-pillared bentonite. *J Hazard Mater* 2011; 186(2-3): 1118-23.
 45. Kerkez Ö, Bayazit ŞS. Magnetite decorated multi-walled carbon nanotubes for removal of toxic dyes from aqueous solutions. *J Nanopart Res* 2014; 16(6): 1-11.
 46. Luo X, Zhang L. High effective adsorption of organic dyes on magnetic cellulose beads entrapping activated carbon. *J Hazard Mater* 2009; 171(1-3): 340-7.
 47. Samiee S, Goharshadi EK. Graphene nanosheets as efficient adsorbent for an azo dye removal: kinetic and thermodynamic studies. *J Nanopart Res* 2014; 16(8): 2542.
 48. Lucia R, Jana S, Ivo Š, Mirka Š, Michaela C, Roman G. Magnetically Modified Tea for Lead Sorption. *Adv Sci Eng Med* 2014;6(4):473-6.